Asian Journal of Chemistry; Vol. 29, No. 10 (2017), 2143-2148

ASIAN JOURNAL OF CHEMISTRY

https://doi.org/10.14233/ajchem.2017.20653

Dielectric Anomalies of $BaTi_{1-x}Fe_xO_3$ Ceramics for x = 0.0 to 0.6 of Fe Doping Concentration

N. GOUITAA*, T. LAMCHARFI, MF. BOUAYAD, F. ABDI, N.S. ECHATOUI and N. HADI

Signals, Systems and Components Laboratory (LSSC), Electrical Engineering Department, Université Sidi Mohamed Ben Abdellah, FST Fez, Imouzzer Road B.P. 2202, Morocco

*Corresponding author: E-mail: najwa.goutaa@gmail.com

Received: 15 March 2017; *Accepted*: 31 May 2017; *Published online*: 31 August 2017; AJC-18508

The $BaTi_{1-x}Fe_xO_3$ ceramics (x = 0.0, 0.1, 0.2, 0.3, 0.4, 0.5 and 0.6) were prepared by the solid state reaction method. The effect of iron substitution on structural and dielectric properties of $BaTiO_3$ ceramic was studied. These compounds are found to crystallize in the mixture of tetragonal and hexagonal phases for $x \leq 0.3$ and only hexagonal phase for $x > 0.3$. Raman spectra indicate that when iron content increases, the intensity of Raman peaks of the tetragonal phase decreases and hexagonal phase grows, which confirm the X-ray results. The dielectric properties of $BaTi_{1-x}Fe_xO_3$ ceramics as function of frequency are studied and showed a relaxation phenomena for pure barium and titanium (BT) (x = 0.0) which is displaced to the higher frequencies accompanied with a decrease in dielectric constant when x increase. The evolution of dielectric permittivity as function of temperature shows a phase transition temperature at Tc = 135 °C for BT and a clear shifting of this temperature to the higher temperature for $BaTi_{1-x}Fe_xO_3$ ceramics.

Keywords: Ceramics, Barium titanate(IV), Structural, Dielectric properties, X-ray diffraction, Raman, Transition temperature.

INTRODUCTION

Tetragonal perovskite barium titanate(IV) ($BaTiO_3$) is a well-known ferroelectric material which was widely used in electronic devices due to it relatively high dielectric constant, electro-optic coefficient and its ferroelectric properties. To produce ferromagnetism ordering in semiconducting $BaTiO_3$ for extending the field of it applications, the 3*d* transition metal can be easily doped and substitute for the titanium atom in BTO due to it close resemblance to the titanium ion in size and valance [1].

The Fe-doped was found to be the most promoting candidate for dilute magnetic oxides (DMO) group due to the presence of magnetic, semiconducting and magnetoelectric coupling properties [2-5]. The barium-site of Ti can be easily substituted by Fe up to 0.7 [6] or higher. It is reported that for less than 0.02 of doping level only tetragonal phase is observed. But, from 0.02 to 0.4 of doping levels mixture tetragonal and hexagonal phase were observed when calcined at 1200 °C and sintered in air at 1250 °C for 2 h [7]. It is generally agreed that doping by Fe ions stabilize the hexagonal phase of $BaTiO_3$ at higher doping levels [8]. However, there are some conflicting reports in the literature about the minimum quantity of Fe needed to stabilize the pure hexagonal $BaTiO_3$ phase. It was also found that the formation of hexagonal phase of Fe-doped $BaTiO_3$ can be achieved by higher sintering temperature and longer sintering time [7].

The aim of this research is to study the influence of Fe on the evolution of structural properties of tetragonal $BaTiO_3$ ceramic at different doping concentration and to understand the ferroelectric behavior of this system. Following this goal, we have synthesize our samples by using solid state method at different doping concentrations (0, 0.1, 0.2, 0.3, 0.4, 0.5 and 0.6). Then the possible structural differences between samples were studied by X-ray diffraction and Raman spectra. To correlate these results with dielectric properties of Fe-doped $BaTiO_3$ ceramics we have studied the dielectric properties of the samples prepared as function of frequency and temperature with an impedance analyzer.

EXPERIMENTAL

The samples were prepared with the solid state reaction method using stoichiometric amounts of $BaCO_3$, TiO_2 and Fe_2O_3. In the first synthesis step the powders were homogenized by milling under acetone according to the formulae of $BaTi_{1-x}Fe_xO_3$, where the doping levels are x = 0, 0.1, 0.2, 0.3, 0.4, 0.5 and 0.6. After 4 h of the milling, the powders were dried at 70 °C for 48 h. The dried powders were mixed using agate mortar and pestle for 0.5 h and then placed in an alumina nacelle for calcination in air at 1100 °C for 4 h. The calcined powders were pressed into pellets and sintered in air for 6 h at 1200 °C. The crystal structure of the product ($BaTi_{1-x}Fe_xO_3$) was characterized by X-ray diffraction (XPERT-

PRO with Cu K_α radiation with λ = 1.5406 Å) and Raman. The dielectric properties as function of frequency and temperature were tested with Agilent E4980A (20 Hz-2 MHz).

RESULTS AND DISCUSSION

XRD study: Fig. 1a shows the XRD patterns of the Fe-doped $BaTiO_3$ ceramics at doping levels of x = 0.0, 0.1, 0.2, 0.3, 0.4, 0.5 and 0.6 calcined at 1100 °C for 4 h. As expected, the $BaTiO_3$ (BT) ceramic without Fe doping showed only tetragonal structure. On the other hand, Fe-doped BT samples have prevailing hexagonal (P63/mmc) crystallographic phase with an admixture of the tetragonal (P4mm) phase for x = 0.1, 0.2 and 0.3. And only the hexagonal phase for doping levels higher than 0.3 [9] with no trace of other impurity phases. To have a better view on the evolution behaviors of the tetragonal and hexagonal phases in the Fe-doped $BaTiO_3$ ceramics, the strongest XRD peaks (101) for the tetragonal phase and (104) for the hexagonal phase are zoomed in the Fig. 1b. The analysis of these peaks reveals that the hexagonal phase become predominant in favour of the tetragonal phase with the increasing in Fe concentration for x = 0.1 to 0.3 while the hexagonal phase is completely formed when x is greater than 0.3.

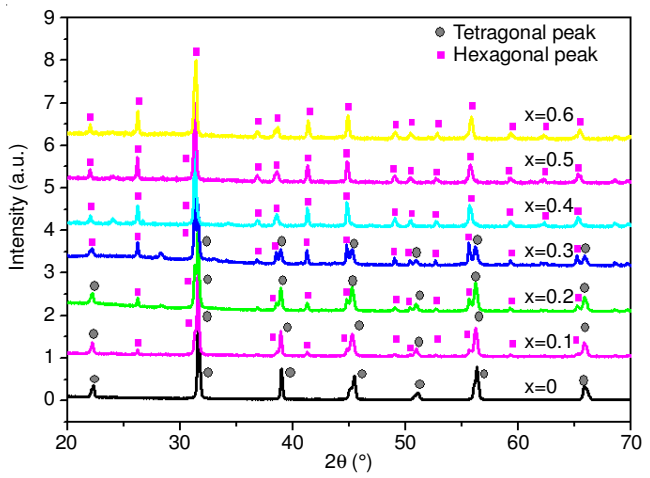

Fig. 1a. XRD patterns of $BaTi_{1-x}Fe_xO_3$ ceramics for x = 0.0, 0.1, 0.2, 0.3, 0.4, 0.5 and 0.6

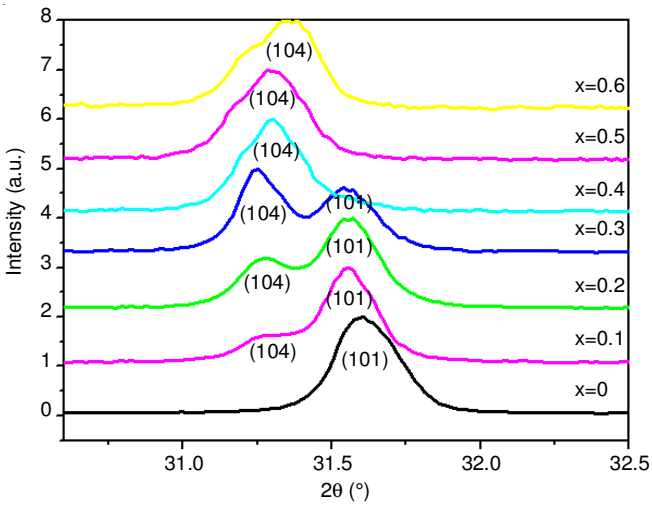

Fig. 1b. XRD peaks (101) for the tetragonal phase and (104) for the hexagonal phase of $BaTi_{1-x}Fe_xO_3$ ceramics for x = 0.0, 0.1, 0.2, 0.3, 0.4, 0.5 and 0.6

There are contradicting reports about the minimum quantity of Fe needed to stabilize the hexagonal phase of BTF ceramics. To identify the parameters responsible for this difference, we have studied the stability of $FeTiO_3$ at different temperature as shown in Fig. 2. The XRD patterns of $FeTiO_3$ oxidized at different temperatures for 4 h show that the $FeTiO_3$ samples are slowly oxidized for temperature range of 600-1000 °C and completely oxidized above 1000 °C for 4 h. This is why the pure hexagonal phase is formed for only 0.06 Fe-doped $BaTiO_3$ reported by Vanderah *et al.* [10] by using multiple one week heatings at 1250-1270 °C as the temperature and the time of this study are higher than 1100 °C/4 h. While Khirade *et al.* [11] found that the tetragonal phase is stable for (x = 0.0 to 0.3) and the mixed phase of the tetragonal and hexagonal structure is stable in the sample with higher Fe concentration (x = 0.4 and 0.5) as the temperature used is 900 °C for 5 h which is lower than the oxidation temperature of $FeTiO_3$. On the other hand, the mixture phases with the same level concentration but synthesis under different conditions of annealing temperature and time were reported [7,12]. These results confirm that the annealing temperature and time are two important parameters for stabilizing the hexagonal phase.

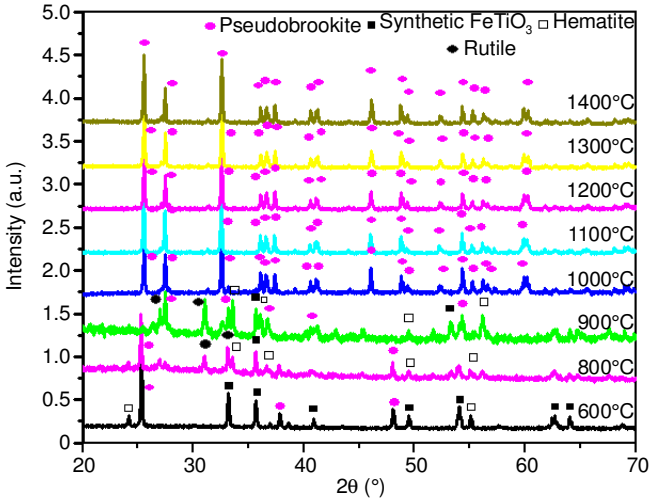

Fig. 2. XRD of $FeTiO_3$ oxidized at different temperatures for 4 h

To understand the effect of annealing temperature on BTF structure, 0.2 Fe-doped $BaTiO_3$ (BTF2) has been treated at different annealing temperature (1100 °C/4 h and 1200 °C/4 h). Fig. 3 shows that at 1200°C the (104) hexagonal peak became stronger than the (101) tetragonal peak. It can be concluded that for less than 0.2 of Fe the temperature needed for stabilization of pure hexagonal phase is higher than 1200 °C/4 h.

The lattice parameters of different compositions in the $BaTi_{1-x}Fe_xO_3$ samples are listed in Table-1. The lattice parameter "a" increases with the increase in Fe doping concentration until x = 0.4 for hexagonal phase and then decreases accompanied with an increase in this parameter for tetragonal phase until 0.3 of Fe concentration. This fact is probably due to the presence of Fe^{3+} with ionic radius [$r_i(Fe^{3+})$ = 0.645 Å] higher than the Ti(IV) ionic radius [$r_i(Ti^{4+})$ = 0.605 Å] for concentration inferior than 0.4. While it is the reverse for x = 0.5, 0.6 and 1.0 due to the presence of Fe^{4+} with the ionic radius [$r_i(Fe^{4+})$ = 0.585 Å] which is smaller than the ionic radius of Ti^{4+} [13].

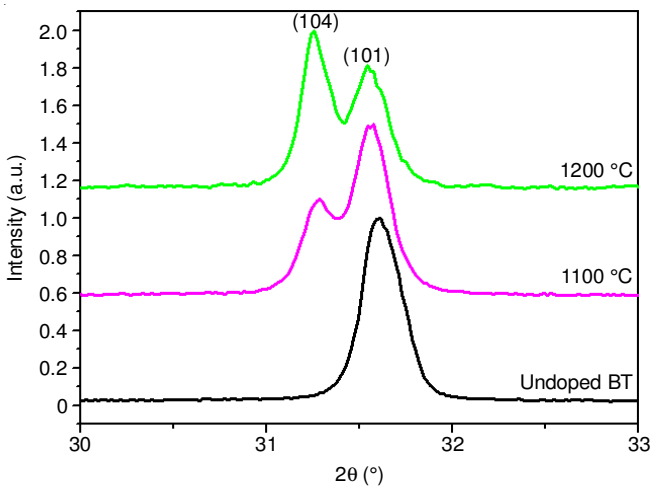

Fig. 3. XRD peaks (101) for the tetragonal phase and (104) for the hexagonal phase of BTF2 (x = 0.2) at 1100 and 1200 °C annealing temperature for 4 h

TABLE-1
LATTICE PARAMETERS OF HEXAGONAL AND TETRAGONAL PHASE OF DIFFERENT COMPOSITIONS OF $BaTi_{1-x}Fe_xO_3$ SAMPLES

Composition of $BaTi_{1-x}Fe_xO_3$	Lattice parameters of hexagonal phase		Lattice parameters of tetragonal phase	
	c (Å)	a (Å)	c (Å)	a (Å)
x = 0.0	–	–	4.2023	3.9908
x = 0.1	12.8486	5.8073	4.0100	4.0031
x = 0.2	12.8458	5.8085	4.0070	4.0062
x = 0.3	12.8446	5.8109	4.0093	4.0060
x = 0.4	12.8169	5.8254	–	–
x = 0.5	12.8086	5.8238	–	–
x = 0.6	12.8022	5.8172	–	–
x = 1.0	12.6725	5.7305	–	–

Raman spectra: Fig. 4 shows the Raman spectra of Fe-doped $BaTiO_3$ ceramics. The Raman spectra of pure BT shows a large and intense bands around 266 and 520 cm^{-1} assigned to the A1 and A1+E(TO) mode respectively. Whereas the broad and asymmetric band around 309 cm^{-1} assigned to the B1+E(LO+TO) mode, is a characteristic peak of tetragonal phase. It confirms the tetragonal phase of pure BT. The band at 719 cm^{-1} is assigned to the A1+E(LO) mode [14].

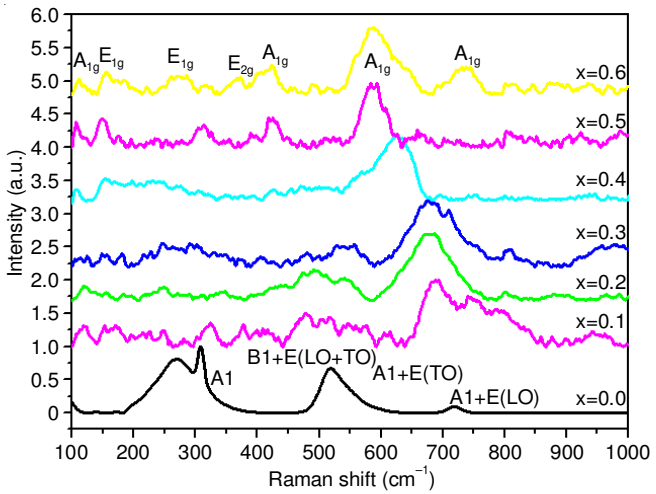

Fig. 4. Raman spectra of Fe-doped $BaTiO_3$ ceramics at different doping concentrations measured at room temperature

With the increasing of Fe content the intensity of the peak at 309 cm^{-1}, characteristic of the tetragonal phase, decreases progressively and disappears completely for concentration higher than 0.3 of Fe, while seven peaks appear at: 115.5, 155, 269.5, 367, 422.5, 588 and 738 cm^{-1}, respectively. According to the Raman spectra of h-$BaTiO_3$ crystals reported by Murugesan *et al.* [15] all these peaks are characteristic of the hexagonal phase. The Raman spectra confirm that the hexagonal phase is stable for 0.3 of Fe content and higher which are in agreement with the X-ray diffraction measurements.

Dielectric constant as function of frequency: The dielectric properties are studied by measuring the dielectric constant dependent on frequency at different temperature as shown in Fig. 5 for $BaTi_{1-x}Fe_xO_3$ with x = 0.0, 0.2, 0.4 and 0.6. For $BaTiO_3$ compound (Fig. 5a), the dielectric constant presents a particular evolution with the increase of frequency. Indeed, ε_r' reaches a maximum with the increase of frequency and then decreases. This maximum value $\varepsilon_{r\,max}'$ increases with the increase of temperature to 6500 for T° = 135 °C and then decrease. For BT ceramic, this maximum $\varepsilon_{r\,max}'$ moved when the temperature changes. In fact, for T° < 135 °C, this shifting take place to the lower frequencies as the temperature of measurement increases. Whereas for temperature above 135 °C, the shifting is to the high frequency. This temperature (T° = 135 °C) is corresponding to the BT transition temperature (Tc), which when it transits from the ferroelectric phase to the paraelectric phase. This evolution of $\varepsilon_{r\,max}'$ with frequency variation is in good agreement with the results reported by Elbasset *et al.* [16]. For Fe-doped $BaTiO_3$ at x = 0.2 (Fig. 5b) we found that the relaxation phenomenon was eliminated or displaced to the high frequencies. And the classical ferroelectric behaviour is observed while the dielectric constant evolution is inversed for the frequencies inferior to 70 KHz (Fig. 5b). This behaviour was displaced to the high frequencies for x = 0.4 and 0.6 (Fig. 5c and Fig. 5d). The Fe substitution eliminates the relaxation phenomenon and decreases the dielectric constant (ε_r') of the samples (Fig. 5b, 5c and 5d). Thus the drastic reductions in ε_r' value upon Fe substitution can be attributed to the creation of oxygen vacancy due to Fe^{3+} ions replacing Ti^{4+} ions. Such oxygen vacancy leads to the breaking of Ti-O bonds and affects the dielectric constant. The same reduction of ε_r' for doping $BaTiO_3$ ceramics is reported by Deka *et al.* [17].

Dielectric constant as function of temperature: The evolution of dielectric permittivity as a function of temperature at different frequencies for pure BT is shown in Fig. 6. The dielectric permittivity if founded to increase with the increasing of temperature and reach a maximum value at 135 °C followed by a decrease. This temperature (Tc = 135 °C) is corresponding to the transition temperature of BT ceramic from the ferroelectric phase to the paraelectric phase.

We have also studied the evolution of dielectric permittivity as a function of temperature at different frequencies of Fe doped BT samples for x = 0.1, 0.2, 0.3 and 0.6 (Fig. 7). There are different anomalies at different temperature for each frequency and a strong dielectric relaxation is observed in all the samples. The relaxation may be ascribed to the polarized nano domains caused by oxygen deficiencies in the samples [2].

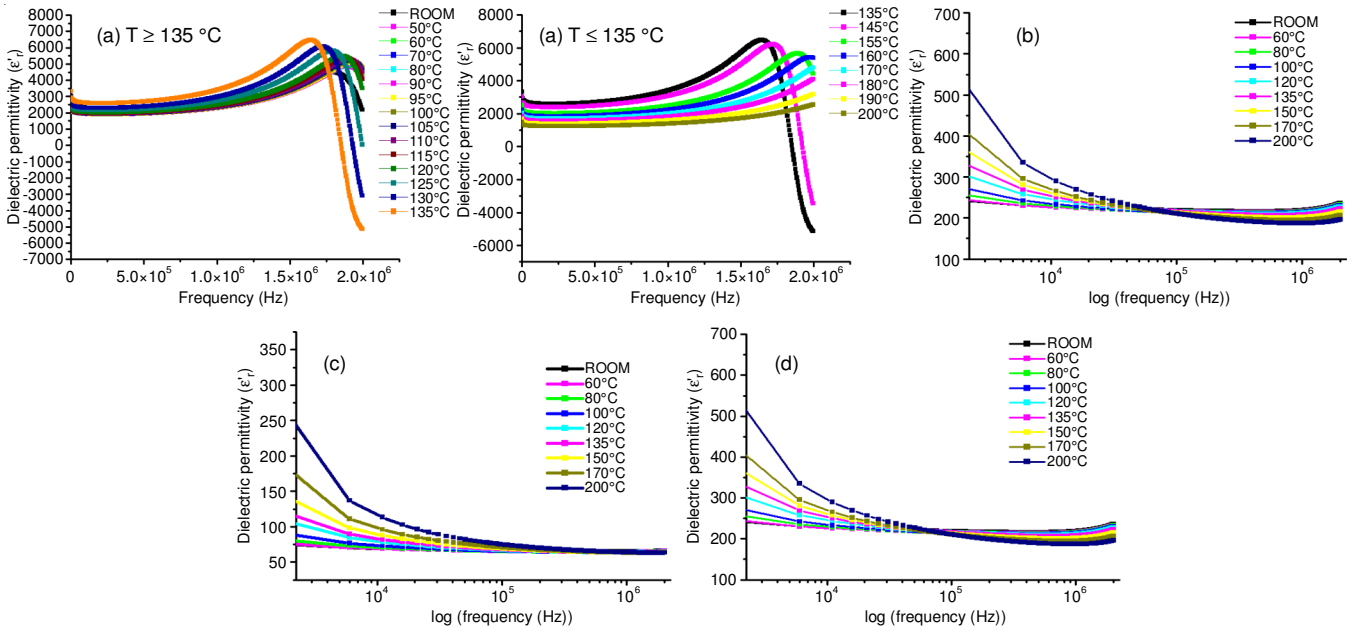

Fig. 5. Dielectric permittivity with frequency variation at different measurement temperatures of BTF samples for (a) x = 0.0, (b) x = 0.2, (c) x = 0.4 and (d) x = 0.6

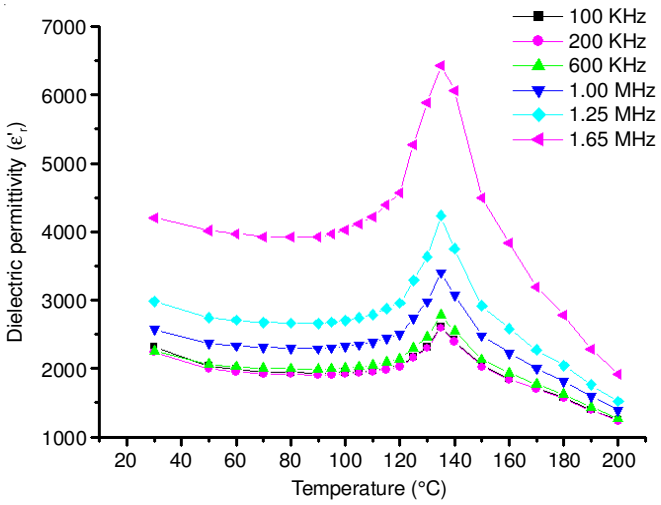

Fig. 6. Temperature dependence of the real part of the permittivity (ε_r') for pure $BaTiO_3$

For downhill of $BaTi_{1-x}Fe_xO_3$, we observed one anomaly at Tc = 200, 250 and 280 °C for x = 0.1, 0.2 and 0.3, respectively (indexed by arrow) which are also present in the up of temperature but decaled to the lower temperature for downhill. The shifting of phase transition to the higher temperature is probably due to the ferromagnetism. However there are several studies which confirm the coexistence of ferroelectricity and ferromagnetism in BTF at low concentration of Fe and only ferromagnetism for high Fe contents [18-20]. The XRD results showed that the hexagonality of BTF samples grows up with the increase of doping concentration inducing ferromagnetism, as the hexagonal phase a well known as a ferromagnetic phase [19], which confirms the Tc shifting. Above 400 °C, a clear increase of dielectric constant was observed in the up and downhill for all the samples which indicates the existence of structural anomaly and it is confirmed at 0.6 of Fe content when ε_r' reaches a maximum at 580 °C. The others anomalies disappear due to the valence fluctuation of Fe^{3+} especially the

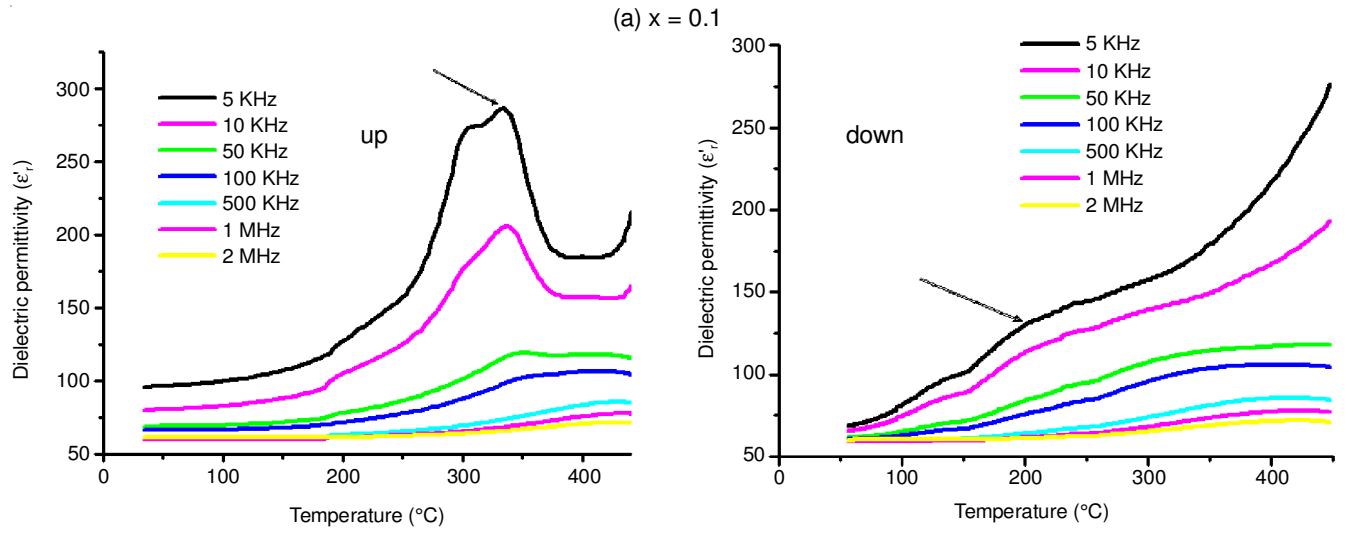

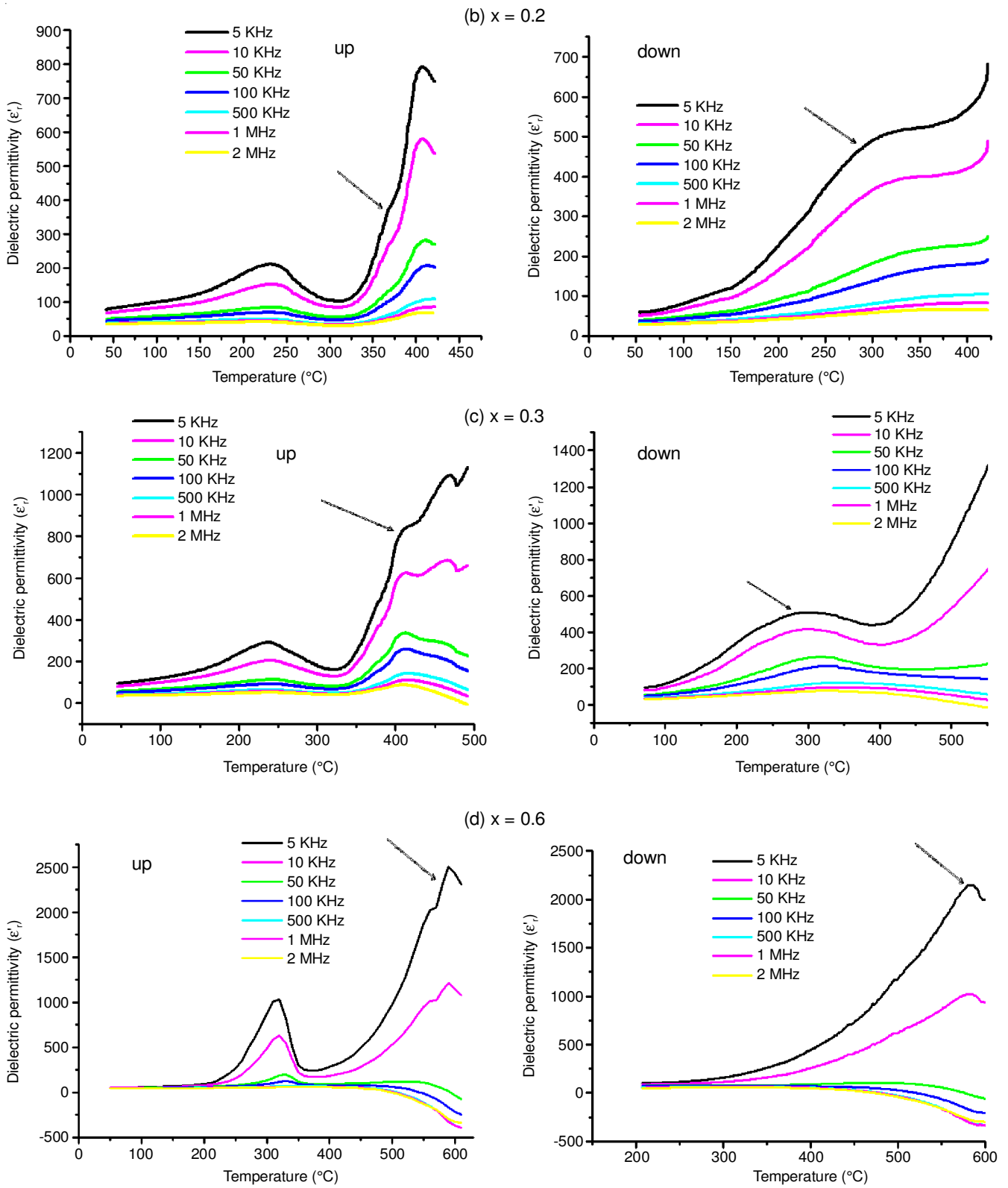

Fig. 7. Temperature dependence of the real part of the permittivity (ε_r') for $BaTi_{1-x}Fe_xO_3$ for (a) x = 0.1, (b) x = 0.2, (c) x = 0.3 and (d) x = 0.6

change from Fe^{3+} to Fe^{4+} ions induced by oxygen vacancies [18].

Conclusion

In this work, $BaTi_{1-x}Fe_xO_3$ samples were synthesized with the conventional solid state method by using $BaCO_3$, TiO_2 and Fe_2O_3 amounts. The $BaTiO_3$ ceramic without Fe-doped levels is found to crystallize in tetragonal phase. The crystal structure of the ceramics changes from the tetragonal phase to the hexagonal phase when the Fe content increase, as it is indicated in both X-ray diffraction and Raman spactra. The evolution of the permittivity as function of temperature for pure BT shows

a phase transition from the ferroelectric phase to the paraelectric phase at Tc = 135 °C. It is found that the doping of $BaTiO_3$ perovskite with Fe contents induce a shifting of phase transition to the higher temperature due to the ferromagnetism generated by hexagonal phase which is stabilized with the increase of Fe concentration and annealing temperature.

REFERENCES

1. D. Hou, Z. Zhou, X. Ye, Q. Zhang, L. Ma and C. Zhen, *Phys. Procedia*, **32**, 498 (2012); https://doi.org/10.1016/j.phpro.2012.03.593.
2. X.K. Wei, Y.T. Su, Y. Sui, Z.X. Zhou, Y. Yao, C.Q. Jin and R.C. Yu, *J. Appl. Phys.*, **102**, 242910 (2013); https://doi.org/10.1063/1.4811699.
3. R. Maier and J.L. Cohn, *J. Appl. Phys.*, **92**, 5429 (2002); https://doi.org/10.1063/1.1510591.
4. A. Rajamani, G.F. Dionne, D. Bono and C.A. Ross, *J. Appl. Phys.*, **98**, 063907 (2005); https://doi.org/10.1063/1.2060945.
5. H. Liu, B. Cao and C. O'Connor, *J. Appl. Phys.*, **109**, 07B516 (2011); https://doi.org/10.1063/1.3556768.
6. F. Lin, D. Jiang, X. Ma and W. Shi, *J. Magn. Magn. Mater.*, **320**, 691 (2008); https://doi.org/10.1016/j.jmmm.2007.08.008.
7. S.Y. Qiu, W. Li, Y. Liu, G.H. Liu, Y.Q. Wu and N. Chen, *Trans. Nonferr. Met. Soc. China*, **20**, 1911 (2010); https://doi.org/10.1016/S1003-6326(09)60394-0.
8. X.K. Wei, Q.H. Zhang, F.Y. Li, C.Q. Jin and R.C. Yu, *J. Alloys Comp.*, **508**, 486 (2010); https://doi.org/10.1016/j.jallcom.2010.08.099.
9. C.F. Chen, G. King, R.M. Dickerson, P.A. Papin, S. Gupta, W.R. Kellogg and G. Wu, *Nano Energy*, **13**, 423 (2015); https://doi.org/10.1016/j.nanoen.2015.03.005.
10. T.A. Vanderah, J.M. Loezos and R.S. Roth, *J. Solid State Chem.*, **121**, 38 (1996); https://doi.org/10.1006/jssc.1996.0006.
11. P.P. Khirade, S.D. Birajdar, A.V. Raut and K.M. Jadhav, *Ceram. Int.*, **42**, 12441 (2016); https://doi.org/10.1016/j.ceramint.2016.05.021.
12. N.V. Dang, N.T. Dung, P.T. Phong and I. Lee, *Physica B*, **457**, 103 (2015); https://doi.org/10.1016/j.physb.2014.09.046.
13. F. Aziz, P. Pandey, M. Chandra, A. Khare, D.S. Rana and K.R. Mavani, *J. Magn. Magn. Mater.*, **356**, 98 (2014); https://doi.org/10.1016/j.jmmm.2013.12.037.
14. W.H. Zhang, L. Chen, Y.T. Tao, W.H. Zhang, J. Chen and J.X. Zhang, *Physica B*, **406**, 4630 (2011); https://doi.org/10.1016/j.physb.2011.09.046.
15. G. Murugesan, R. Nithya and S. Kalainathan, *Int. J. ChemTech Res.*, **6**, 1633 (2014).
16. A. Elbasset, Ph.D. Thesis, Synthèse et caractérisation des matériaux céramiques de $BaTiO_3$ purs et dopés au strontium et au zirconium, Université Sidi Mohamed Ben Abdellah, Fez, Morroco (2014).
17. B. Deka, S. Ravi, A. Perumal and D. Pamu, *Physica B*, **448**, 204 (2014); https://doi.org/10.1016/j.physb.2014.03.069.
18. I.N. Apostolova, A.T. Apostolov, S.G. Bahoosh and J.M. Wesselinowa, *J. Appl. Phys.*, **113**, 203904 (2013); https://doi.org/10.1063/1.4807412.
19. B. Xu, K.B. Yin, J. Lin, Y.D. Xia, X.G. Wan, J. Yin, X.J. Bai, J. Du and Z.G. Liu, *Phys. Rev. B*, **79**, 134109 (2009); https://doi.org/10.1103/PhysRevB.79.134109.
20. D.P. Dutta, M. Roy, N. Maiti and A.K. Tyagi, *Phys. Chem. Chem. Phys.*, **18**, 9758 (2016); https://doi.org/10.1039/C5CP07736B.